THE INFLUENCE OF RIVETING PROCESS ON SHEETS FATIGUE LIFE – THE STRESS STATE ANALYSIS

Elżbieta SZYMCZYK*, Jan GODZIMIRSKI**

* Department of Mechanics and Applied Computer Science, Faculty of Mechanical Engineering
** Institute of Aviation Technology, Faculty of Mechatronics and Aeronautical
Military University of Technology, ul. Kaliskiego 2, 00-908 Warszawa, Poland

eszymczyk@wat.edu.pl, jgodzimirski@wat.edu.pl

Abstract: The paper deals with estimation of a stress concentration factor in the hole area during tensile loading. The load carrying capacity and fatigue performance of sheet samples (made of 2024 aluminium alloy) with open and riveted holes are compared. Tests confirm the insignificant influence of riveting on ultimate strength, however, it strongly affects fatigue life. The material cold working around the hole causes a decrease in maximum principal stress values as well as stress concentration moves away a few millimetres (about half a rivet radius length) from the hole. During tensile loading the maximum stress values increase slower around the riveted hole than at the open one and consequently in the former case the yield stress is achieved later.

Key Words: Riveted Joints, Residual Stress States, FEM Analysis

1. INTRODUCTION

The object of analysis are riveted joints used in aircraft structures to fasten skins with the frame. High-strength aluminium alloys 2xxx (with copper) or 7xxx (with zinc) are thought of as the aircraft alloy because of their strength and excellent fatigue resistance however the copper content makes them extremely difficult to weld. The tens or even hundreds of thousands rivets used in a typical aircraft structure have a significant influence on the service life and this is the reason of the last decades research concerning fatigue performance improvement.

The load carrying capacity and fatigue resistance of riveted joints depends on many structural, manufacturing and material factors (Szulżenko and Mostowoj, 1970; Godzimirski, 2008; Matwijenko, 1994; Jachimowicz and Wronicz, 2008) like: connection type (overlap or butt, symmetric or asymmetric), size, rivet pitch and spacing (distance between rivets and rivet rows), sheet thickness, diameter of rivet shank and rivet type (i.e. universal, mushroom or countersunk). The most advantageous stress states occur for symmetric joints (where uniaxial or biaxial tension is dominant). Unfortunately, they can be rarely used in practice. The non-symmetric joint is very unfavourable because of eccentric tension (secondary bending). The secondary bending influence is estimated by comparing maximum bending stress in the concentration area with the nominal stress in the reduced section or with local tension stress. In the paper a uniaxial tension of the sheet with an open and riveted hole are analysed. The values and fields of principal stress obtained for this case provide a base of more accurate evaluation of the other factors (e.g. secondary bending) influence on fatigue life.

The manufacturing factors include mainly: a method and quality of riveting (hole drilling, finishing the edges, concentricity of holes in joining sheets and rivet squeezing) (Gruchelski et al., 1969; Godzimirski, 1998; Szymczyk and Jachimowicz, 2007; Szymczyk, 2010; Deng and Hutchinson, 1998; Muller, 1995; Rans, 2007). Static cold riveting (with a press) or dynamic (with a pneumatic hammer) are used to assemble components of an aircraft fuselage. A residual stress state in the joint results from the riveting process. Despite local exceeding of the yield stress, it has a profitable influence on fatigue performance. In this paper the influence of residual stress (regarding the various magnitude of squeezing force) on the stress fields during tensile loading is analysed.

The calculations are performed for sheets with open holes and riveted ones. Two types of the hole shape are analysed: cylindrical one and with a conical socket for a countersunk (flush) rivet. Countersunk rivets are used for external surfaces of an aircraft, which airspeed is higher than 300 km/h, in order to reduce aerodynamic resistance. The theoretical case of symmetric squeezing is analysed for the sheet with a cylindrical hole to obtain the most profitable - uniform stress distribution around the hole (Abibow, 1982). The actual stress state is nonuniform; higher values of stress are in the sheet on the driven rivet head side (Szymczyk, 2010; Rans, 2007).

For an aircraft purpose sheets of thickness from 0.6 mm to 4 mm are used. In the paper a sheet of 2 mm thickness and rivet of 4mm diameter (mushroom and countersunk) are analysed. Aluminium alloys 2024T4 for sheets and PA24 (corresponding to 2117) for rivets, widely used in aircraft industry, are undertaken in the paper. The load carrying capacity of sheets depends on rolling direction (the difference can reach 5%). This condition is not concerned in numerical models where isotropic materials are assumed.

Riveted joints are areas of stress concentrations where crack initiation of an aircraft fuselage is likely/tends to start (Rans, 2007; Kocańda et al., 2007; Howland, 1930; Hartman, 1961). The aim of this paper is analysis of stress state around the hole in the sheet with regard to rivet type and residual stresses and their influence on fatigue performance of sheets. Stress concentration magnitude is estimated in the hole area during tensile loading as a result of the numerical calculations.

2. EXPERIMENTAL TESTS

The static tension test of 2024T4 aluminium alloy used in aircraft fuselages is carried out to obtain the stress-strain curve (Fig. 1). Yield strength is of 330 MPa. The values of real stress are calculated using the experimental data (with respect to the decreasing of specimen cross section during tension) and the following well known formula: $\sigma_{rz} = \sigma(1+\varepsilon)$.

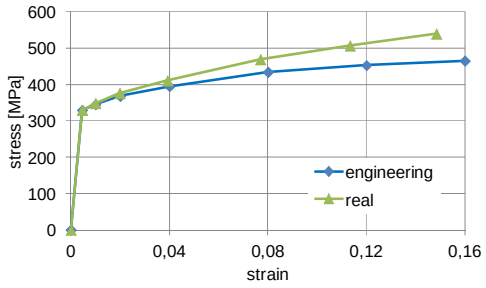

Fig. 1. Stress-strain curves for aluminium alloy 2024T4

Afterward, the sheet samples of 2mm thickness, 30 mm width and 170 mm length with centrally localised hole of 4 mm diameter are made of 2024T4 alloy. Some samples are prepared for countersunk rivets with angle of 90º [BN 70/1121-03] using a spotting drill. The load carrying capacity of such samples is estimated and compared with ultimate tensile strength of a sample without a hole. The applied tensile stress and the nominal stress in the reduced cross section for cylindrical and countersunk holes are compared in Tab. 1.

Tab. 1. The load carrying capacity for samples of 1.99 mm thickness

specimen type	without hole	cylindrical hole	hole with socket
applied stress [MPa]	445 ± 6	336 ± 12	327 ± 11
nominal stress [MPa]	445	388	394

Tab. 2. Fatigue life of samples with open holes for applied stress range of 134 MPa

sample number	hole type	number of cycles
p1	cylindrical	65 296
p2	cylindrical	77 773
p3	cylindrical	72 306
p4	with socket	63 992
p5	with socket	56 452
p6	with socket	61 264

The samples with holes are subjected to cyclic tension with an applied stress range from 3 to 134 MPa and frequency of 20 Hz. Fatigue life (number of cycles to damage) is presented in Tab. 2.

Subsequently, the samples with holes riveted using mushroom or countersunk rivets are prepared and subjected to fatigue load (Tab. 3). For all samples with mushroom rivets the crack initiation starts in a full cross section at some distance from the hole (Fig. 2). Fatigue life for samples with countersunk rivets is over three times lower than for mushroom ones, however, nearly two times higher than for samples with open holes. The cracks propagate through the reduced section in the latter cases.

Tab. 3. Fatigue life of samples with riveted holes

nr	rivet type	applied stress [MPa]	nominal stress [MPa]	number of cycles
n1	mushroom	3 … 134 3 … 200	155 232	340 000 + 255 176
n2	mushroom	3 … 167 3 … 200	193 232	276 000 + 109 883
n3	mushroom	3 … 200	232	422 000
n4	countersunk	3 … 200	242	131 046
n5	countersunk	3 … 200	242	100 680
n6	countersunk	3 … 200	242	117 863

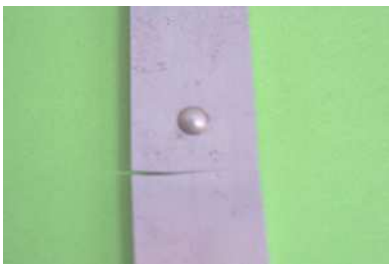

Fig. 2. Fatigue crack of the sheet with a hole riveted with mushroom rivet

The influence of rivet squeezing on the load carrying capacity of the sheet with a hole is also examined. The results of the test are presented in Tab. 4. It is possible to observe that squeezing of the rivet has no effect on ultimate tensile strength but increases the fatigue performance of such sheets.

Tab. 4. The load carrying capacity of riveted sheets

Sample type	with mushroom rivet	with countersunk rivet
applied stress [MPa]	336 ± 8	328 ± 14
nominal stress [MPa]	388	396

3. NUMERICAL MODELS

3D numerical models of the samples described in the previous section are prepared using Patran. Finite element meshes of the rivet neighbourhood in the sheets for countersunk and cylindrical holes are presented in Fig. 3. The case of theoretical symmetric riveting is considered for a cylindrical hole to achieve the most beneficial uniform stress field in the sheet. One half of the sheet is modelled due to plane symmetry with respect to its middle surface. The rivet and sheets models consist of eight-noded, isoparametric solid elements with a tri-linear interpolation function and eight integration points. A rounded mesh shape and small elements close to the rivet holes and larger elements a bit further from the rivet region are taken into account. The calculations are carried out with Nastran and Marc codes.

The specimens are made of aluminium alloy 2024T3 used in aircraft structures and rivets are made of PA24 alloy (corresponding to 2117). The nonlinear elasto-plastic material models are taken into consideration. The stress-strain curves (obtained from a compression test of the rivet sample and tension of the

sheet one) are shown in Fig. 4. The yield value for the multiaxial state is calculated using the von Mises criterion.

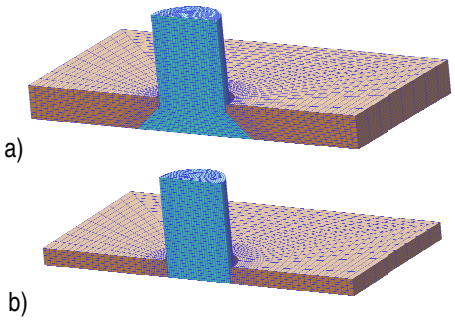

Fig. 3. Models of rivet neighbourhoods: a) countersunk hole, b) cylindrical one.

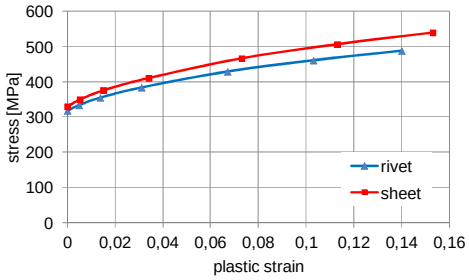

Fig. 4. Material stress-strain curves

The classical updated Lagrange formulation (with large strain plasticity option) for elastic–plastic materials is used due to large geometrical and material nonlinearities.

The riveting tools (bucking bar and punch/riveter) are described using rigid elements. Contact with friction is defined between the mating parts of the joint. The Coulomb model with trial friction coefficient $\mu = 0.2$ is used. The penalty method is applied to implement numerically the contact constraints. The contact stiffness is proportional to stiffness of mating elements and their sizes.

The iterative penetration checking approach allows changing of the contact condition within the Newton-Raphson iteration loop. Using this procedure, the iteration process is done simultaneously to satisfy both the contact constraints and global equilibrium.

Degrees of freedom, corresponding to grip condition in the testing machine, are fixed on each end of the sheets. Additionally, in the latter model (with cylindrical hole), degrees of freedom related to the plane symmetry are fixed in normal direction.

Two steps of loading are carried out. In the first step, corresponding to the rivet squeezing, the bucking bar is fixed and punch is driving to achieve shop (driven head) diameter according to riveting standards. Afterwards, the riveting tools are removed. In the second step the sample is tensile loaded. In the case of samples with open holes only the latter step is done.

4. NUMERICAL ANALYSIS

The aim of the paper is to explain the influence of riveting on the fatigue life of the sample with a hole. The rivet affects it in two ways. The rivet as a rigid element filling the hole restricts its deformations and, as a result, limits the decreasing capacity of the diameter. Moreover, during riveting the sheet material around the hole is squeezed (cold worked) what leads to its hardening (the yield stress increase in cyclic loading). The numerical FE analysis is performed for the sheets with mushroom and countersunk rivets in order to estimate the influence of these factors on the growth in fatigue life of the sample. The material effort in terms of fatigue life is better described by the 1st principal stress than Huber-Mises equivalent stress.

In the first step, the analysis of the sheet with a cylindrical hole is performed. The comparison of a stress state for an open hole and a hole with a rivet shank set inside, both loaded with 184 MPa, is shown in Fig. 5. The calculations confirmed that filling the hole with a rivet shank (without squeezing) has a negligible influence on the maximum stress level at the rivet hole. Otherwise, material cold working around the rivet hole causes about 20% reduction of the principal stress maximum value in this area. Stress concentration still occurs in the reduced hole cross section, however, no longer takes place exactly/strictly at the hole edge.

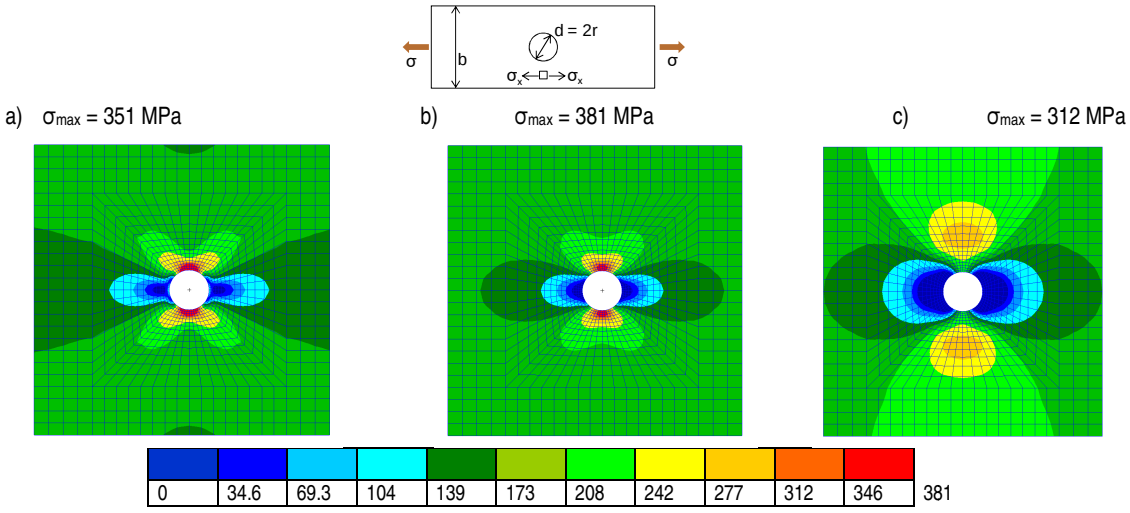

Fig. 5. Principal stress fields close to the rivet hole: a) sheet with an open hole b) with a rivet shank set inside the hole (without squeezing) c) with an upset rivet and with consideration of material hardening (residual stress state due to riveting)

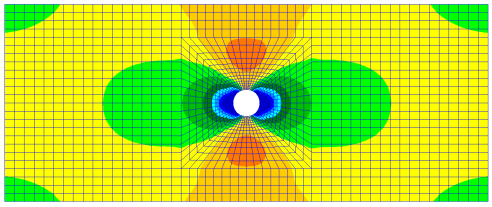

Fig. 6. The σ_1 stress field in the sample with an upset rivet (the same scale as in Fig. 5)

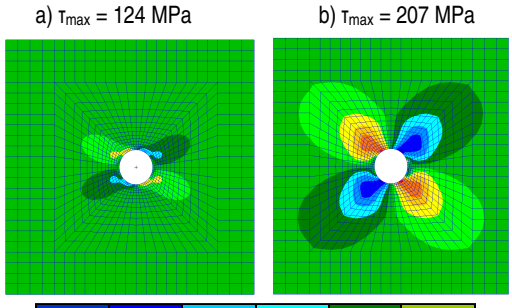

Fig. 7. The shear stress fields: a) sample with an open hole b) sample with an upset rivet

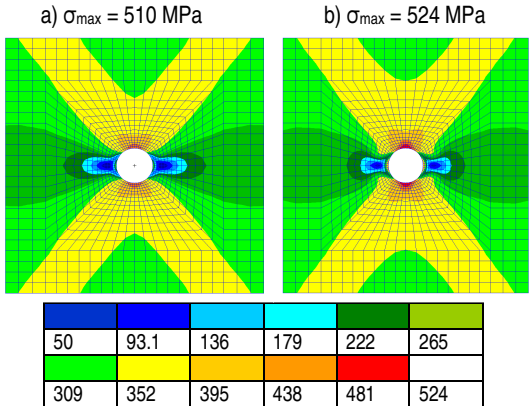

Fig. 8. Equivalent stress fields: a) specimen with an open hole b) specimen with a riveted hole

The principal stress values (334 MPa) exceed the yield stress as a result of increasing applied stress to 244 MPa, whereas the stress distribution (Fig. 6) remains nearly the same as in elastic range (Fig. 5c).

The shear stress fields in the sample with the open hole and with the riveted one (for an applied stress 184 MPa) are shown in Fig. 7. Analysis of the principal and shear stress states presented in Fig. 6 and 7, respectively, leads to the conclusion that a crack tends to initiate from the specimen free edge (in the area showed in Fig. 2), especially if an existence of positive normal stresses in this area of the sample edged by milling is considered.

There are not observed any important differences in equivalent stress states between the sample with the open hole and the riveted one subjected to ultimate stress equal to 360 MPa (Fig. 8). This result is in good accordance with tests during which load carrying capacity of both samples (with an open and riveted hole) is determined to be at the same level.

The aim of the above stress analysis for the selected load levels is qualitative explaining of the increase in fatigue life of riveted samples in comparison to samples with open holes but first of all pointing out the reason of crack initiation movement from the reduced cross section.

Secondly, quantitative analysis of changes in principal stress (equal to σ_x component in load direction) is performed during tension of the sample with an open and riveted cylindrical hole. The normalised stress values (related to sheet yield stress R_e) are presented in the below figures to simplify the comparison among various models. The comparison of stress values as well as places of their concentration in the hole cross section are marked in Fig. 9.

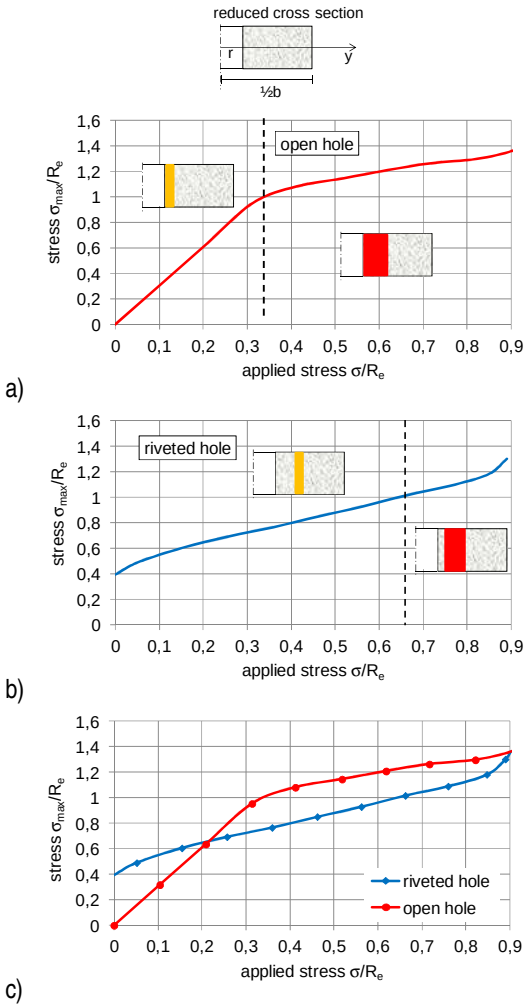

Fig. 9. Principal stress graph vs. applied stress in sheet with cylindrical hole: a) open hole c) riveted hole c) comparison

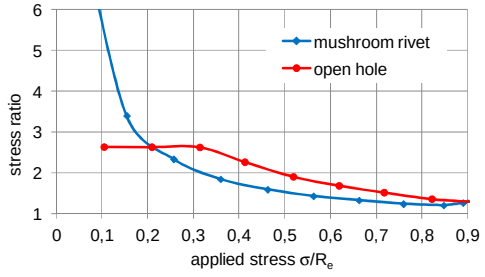

Fig. 10. Stress concentration graph for sheet with cylindrical hole vs. applied stress

The maximum principal stress values for the sheet with an open hole exceed the yield stress for applied stress of 33% R_e, while for the sheet with a riveted hole, due to residual stresses, the increase in principal stress values is remarkably slower (over seven times slower than for an open hole sample). Consequently, the yield stress is obtained for the applied stress level of 66%R_e (two times greater than in former case). The increase in maximum principal stress values (for the sheet with riveted hole) is uniform in almost the whole range of loading. The exceeding of the yield stress has no effect on the maximum stress growth rate. Only in the last stage of loading, when the hole cross section is in the plastic state (nominal stress values in this section reach the yield stress level), principal stresses change faster.

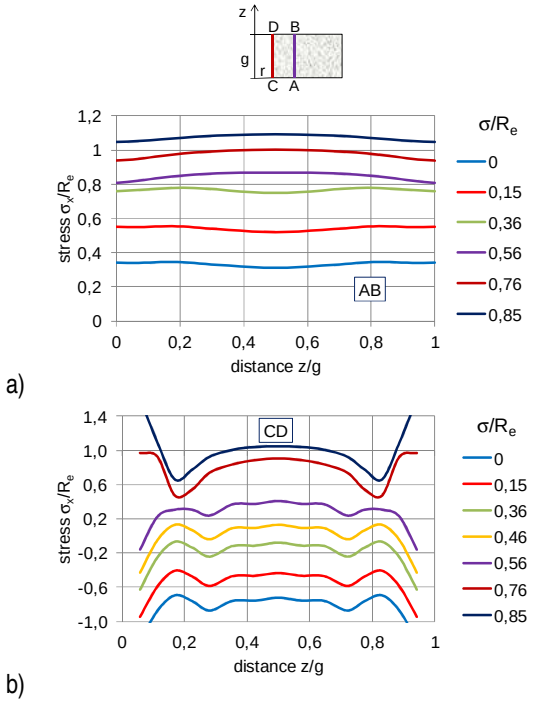

Fig. 11. Principal stress graph vs. thickness distance and applied stress for riveted sample: a) 4 mm from hole axis b) at the edge of the hole

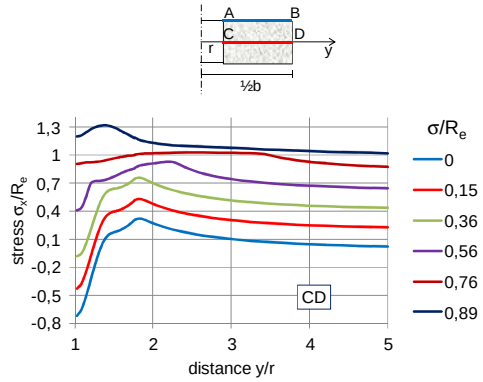

Fig. 12. Principal stress graphs vs. tensile load and distance from the hole axis for riveted sample

In the elastic stage of tensioning the stress concentration (maximum stress value related to nominal stresses in reduced section) for the sheet with an open hole is equal to 2.64 and for assumed dimensions of sheets is in very good accordance with the analytical value (Howland, 1930). After exceeding the yield stress value of the coefficient gradually decreases. The initial stress concentration value approaches infinity for a riveted sample since the nominal applied stress value is equal to zero while residual principal stress is greater than zero. The stress concentration magnitude decreases rapidly while the load increase and for applied stress of 20% R_e reaches the same value as for an open hole, then it still decreases and remains below the corresponding value for an open hole.

During tensile loading in the stress concentration area the principal stress axis is the same as load direction therefore the maximum principal stress (σ_I) is equal to σ_x component.

The principal stress (σ_x component) values for symmetrical riveting are practically constant in the whole reduced section (Fig. 11a). Small distortions only occur at the edge of the hole.

The maximum residual stress (after squeezing) occurs not at the edge of the hole but inside the sheet material, at half the radius length from the edge approximately. During tensile loading the distance from the edge to the stress concentration area even increases (Fig. 12). The stress graph on the outer surface (section AB) changes similarly to those on the middle one (section CD) but under a driven head is less regular.

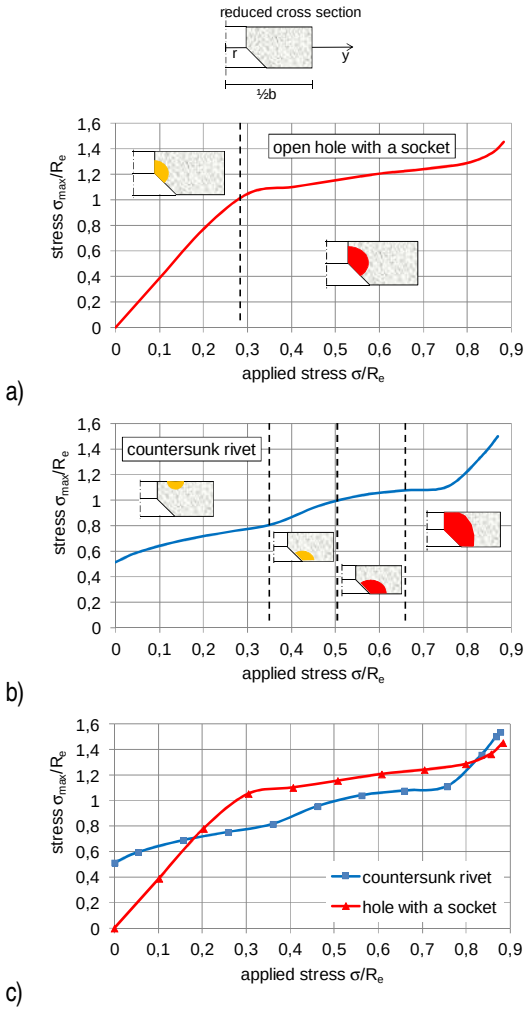

Fig. 13. Principal stress graph vs. applied stress in sheet with countersunk hole: a) an open hole c) riveted hole c) comparison

At the next stage, the calculations for a sheet with a countersunk hole are performed to make a comparison with a cylindrical one. The Maximum principal stress diagrams versus applied load for a sheet with a countersunk hole (open and riveted) are shown in Fig. 13. Principal stress for a sheet with an open hole exceeded yield stress for applied stress of 27% R_e. The growth of principal stresses for the riveted hole (due to residual stresses) is much slower (seven times than for an open one) and, as a result, the yield stress is reached for applied stress of 50% R_e (almost two times greater than in former case). Stress concentration occurs at the edge of the hole in the area where a cylindrical part turns into a conical one (Fig. 13a). The growth of maximum principal stress for the sheet with a riveted hole is relatively uniform almost in the whole analysed load range but for applied stress between 34% R_e and 66% R_e graph becomes slightly irregular what is connected with the change of the stress field in the reduced cross section (the stress concentration area moves from the sheet surface on the driven head side to the outer edge of the conical part of the hole) (Fig. 13b).

The coefficient of stress concentration (Fig. 14) for the sheet with a countersunk riveted hole is lower than a corresponding value for an open hole (practically in the whole load range) what is similar to results obtained for a cylindrical hole.

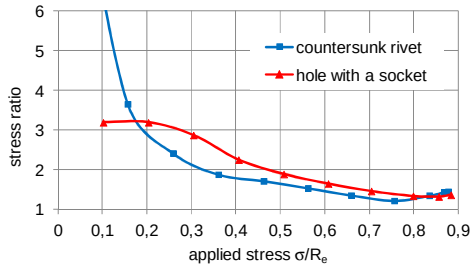

Fig. 14. Stress concentration graph for sheet with countersunk hole vs. applied stress

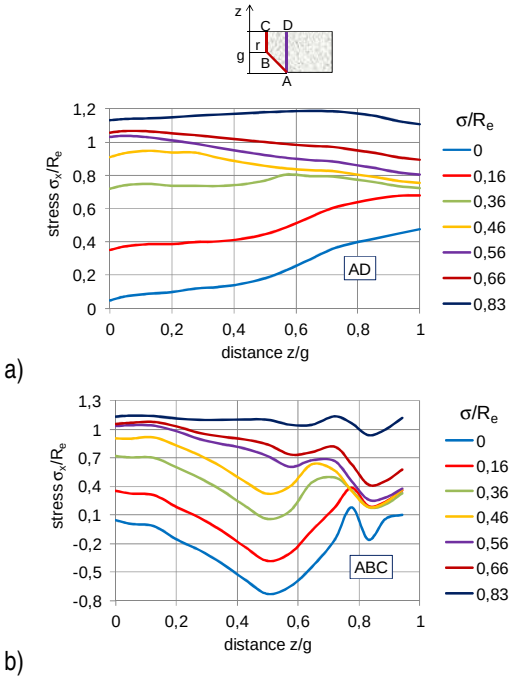

Fig. 15. Principal stress graph vs. thickness distance and applied stress for a riveted sample: a) 3.5 mm from the hole axis b) at the edge of the countersunk hole

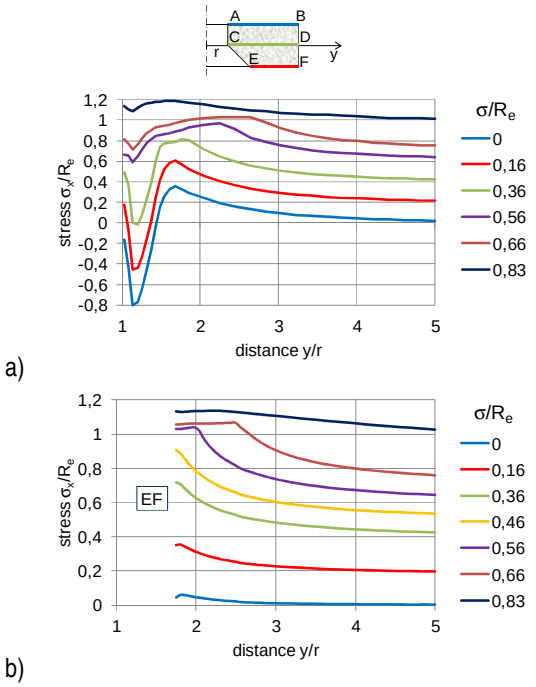

Fig. 16. Principal stress graphs vs. distance from the hole axis and applied stress for riveted sample (countersunk rivet)

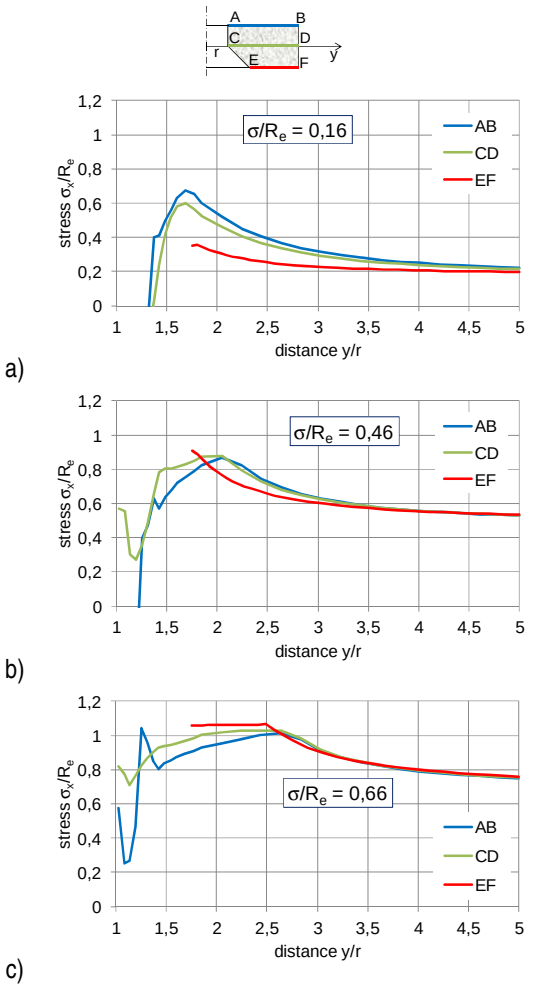

Fig. 17. Principal stress graphs vs. distance from the hole axis for riveted sample (countersunk rivet) for selected applied stress levels: a) 16% R_e, b) 46% R_e, c) 66% R_e

A conical shape of the socket in the hole has an important influence on the principal stress state (Fig. 15). After squeezing, the stress concentration occurs on the sheet surface on the driven head side (D point). During tensile loading (for applied stress of 36% Re) a change in stress field appears. The stress concentration area is being moved to a conical part of the hole (A point). The most irregular stress state is recognised at the edge of the hole under the driven head (Fig. 15b)

Similarly as for a cylindrical hole, the stress concentration occurs not at the edge of the hole but inside material approximately at half the radius length from the cylindrical edge (Fig. 16a). During tensile loading the stress concentration area is being moved to the conical part of the hole (Fig. 16b and 17). Stress values on the outer surface of the sheet (section AB) change similarly as on the middle surface (section CD) but under a driven rivet head (point A) negative stress values (compression) are nearly two times larger.

The comparison of principal stress values for the cylindrical hole and for the hole with a socket is shown in Fig. 18. In the elastic range maximum values of principal stress are a few percent higher for the hole with a socket, what is a result of a smaller area of the reduced cross section. The principal stress values over the yield stress for an open hole are practically independent on the shape of the hole. However, for a riveted hole the corresponding curves are almost parallel in the whole load range. Slight irregularities can be observed for applied stress from 35% to 65% of the yield stress, in this scope for the hole with a socket the change in stress state occurs - the stress concentration appears at the edge of the hole in the conical part (Fig. 13).

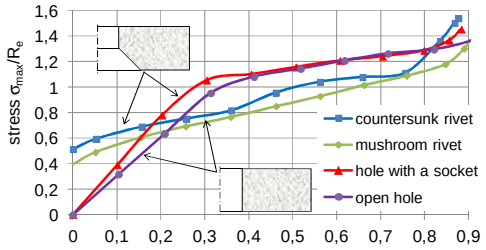

Fig. 18. The comparison of principal stress for samples with cylindrical and countersunk hole

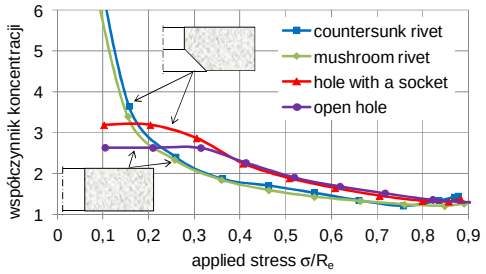

Fig. 19. The comparison of stress concentration for samples with cylindrical and countersunk hole

The stress concentration (Fig. 19) for riveted holes only slightly depends on the shape of the hole while for the hole with a socket is a bit higher (about 1%). The concentration coefficient for the sheet with an open hole within the elastic range is about 20% higher for the hole with the socket. However, it is almost at the same level for both the hole types over the yield stress.

The analysis of the stress concentration coefficient (Fig. 19) does not provide a sufficient information about the state of a riveted joint with regard to the results of fatigue tests (presented in chapter two). Much more information can be obtained from the principal stress graph (Fig. 18). It seems to be especially important to compare these values with the yield stress, but only analysis of stress fields for a selected applied stress level can be used for a deeper insight on fatigue performance.

Fatigue tests of sheets with open holes are carried out at applied stress of 40% R_e. The maximum principal stress for a cylindrical hole and a hole with a socket at this load level are practically the same and over the yield stress (110% R_e). This is the reason for comparable low fatigue life of this sheets. It can be observed in Fig. 18 that for applied stress of 30% R_e fatigue life of the sheet with a cylindrical hole should remarkably increase.

Tests for sheets with riveted holes are performed at applied stress of 40% R_e. According to Fig. 18, it leads to maximal principal stress lower than the yield stress – 80% R_e, what suggests high cycle fatigue strength confirmed in tests. Secondly, tests at applied stress of 60% R_e are performed causing damage of samples with countersunk rivets. The maximum principal stress for this load level is above the yield stress (106% R_e) as it can be read in Fig. 18 and stress concentration appears at the hole surface (Fig. 13b) what suggests slightly higher fatigue life than for a sheet with an open hole (in experiments almost two times higher). The damage character for samples with a mushroom rivet is different than for other cases. The failure does not appear in the reduced section. In this case the maximum principal stress level is about 96% R_e (lower than yield stress) as it can be observed in Fig. 18, however, it seems to be more important that stress concentration occurs inside sheet material at a remarkable distance from the hole (longer than hole radius).

The residual stress state is a significant feature of a riveted sheet. It depends on squeezing force (and driven head diameter). Accordingly to riveting standards the driven head diameter should be equal to 1.5d with tolerance of 0.1d, where d is a rivet shank diameter. The diagram of maximum principal stress (for a driven head diameter of 1.4d ,1.5d and 1.6d) during tension tests is shown in Fig. 20. The increase in squeezing force, estimated from a driven head diameter, leads to the increase in residual stress nevertheless the higher residual stress values the increase rate of principal stresses is slower. As a result, with the increase of driven head diameter (from 1.4d to 1.6d) principal stress values reach the yield stress level at applied stress of 44 % R_e ,50% R_e and 60% R_e, respectively. At the first stage of tensile loading, the maximum principal stress values increase with the increase of a driven head diameter. The situation is entirely opposite for the applied stress of 30% R_e and higher. As assumed, the maximum residual stresses (corresponding to the driven head diameter of 1.6d) proved to be the most advantageous.

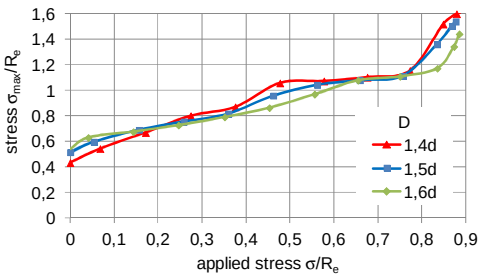

Fig. 20. Principal stress graph vs. driven rivet head diameter (squeezing force)

5. CONCLUSIONS

Filling the hole with a squeezed rivet has no effect on the ultimate strength of the sheet with a hole, however, it remarkably increases its fatigue life.

The material cold working as a result of riveting is the main reason for the fatigue life growth of riveted samples. The performed tests and calculations allow the conclusion that the localization of the crack initiation at the sheet edge is not only a result of the stress state, but also depends on sheet width and most of all on existence of a free surface at the edge of the sheet.

Numerical calculations allow the estimation of maximum stress values close to the notch and consequently the stress concentration magnitude (which is the base of fatigue life estimation of parts with notches [3,9]) for various stress amplitudes of a fatigue cycle.

The material effort in terms of fatigue life is better described by the 1st principal stress than by Huber-Mises equivalent stress. The analysis of the maximum principal stress values during tensile loading allows the evaluation of the influence of different factors (like shape of the hole, residual stress state, applied load) on fatigue life of the sheets.

The equivalent residual stress values in the hole neighbourhood obtained from squeezing exceed the yield stress. On the other hand, the 1st principal stress magnitudes are at the level 50-60% R_e and what is more important they are moved from the hole surface inside material volume. During tensile loading, the growth of the maximum principal stress values is considerably slower for the sheet with a riveted hole and consequently they reach the yield stress level later (for higher applied load).

The 1st principal stress graph versus the applied stress provides more information than the graph of the stress concentration magnitude, however, only the stress state analysis for selected levels of applied load allow the localization of the crack initiation point and a deeper insight on fatigue performance.

REFERENCES

1. **Abibow A.Ł.** (1982), *Technołogia samoletostrojenia*, Moskwa Maszinostrojenie.
2. **Deng X., Hutchinson J.W.** (1998), The clamping stress in a cold driven rivet. *Int. J. Mech. Sci.,* 40, 7, 683-694.
3. **Godzimirski J.** (1998), *Naprawa płatowców*, WAT Warszawa.
4. **Godzimirski J.** (2008), *Lotnicze materiały konstrukcyjne*, Warszawa WAT.
5. **Gruchelski B., Szumielewicz K., Wanad T.** (1969), Przegląd i naprawa sprzętu lotniczego, *Wydawnictwo Komunikacji i Łączności* Warszawa.
6. **Hartman A.** (1961), *Some tests on the effect of fatigue loading on the friction in riveted light alloy specimens*, NLR M2008, NLR, Amsterdam.
7. **Hartman A., Schijve J.** (1969) *The effect of secondary bending on the fatigue strength of 2024-T3 Alclad riveted joints*. NLR TR 69116U, NLR, Amsterdam.
8. **Howland R.C.J.** (1930), On the stress in the neighbourhood of a circulair hole in a strip under tension, *Phil. Trans. of the Roy. Soc.*, Series A (229), London, 49–86.
9. **Jachimowicz J., Wronicz W.** (2008), Wybrane problemy modelowania nitowych lotniczych struktur cienkościennych, *Przegląd Mechaniczny* LXVIII nr 5.
10. **Kocańda D., Hutsaylyuk V., Hlado V.** (2007), Analiza rozwoju małych pęknięć zmęczeniowych od otworu oraz mikromechanizm pękania platerowanej blachy ze stopu 20024-T3, *Biul. WAT* Vol. LVI Nr 4.
11. **Matwijenko W.A.** (1994), Wpływ czynników konstrukcyjno-technologicznych na wytrzymałość zmęczeniową połączeń klejowo-nitowych, *Technologia i Automatyzacja Montażu* Nr 2.
12. **Muller R.** (1995), *An experimental and numerical investigation on the fatigue behaviour of fuselage riveted lap joints*, Doctoral Dissertation, Delft University of Technology.
13. **Rans C.D.** (2007), *The Role of Rivet Installation on the Fatigue Performance of Riveted Lap Joints*, Department of Mechanical and Aerospace Engineering Carleton University.
14. **Rijck J.** (2005), *Stress Analysis of Fatigue Cracks in Mechanically Fastened Joints*, Doctoral Dissertation, Delft University of Technology
15. **Szulżenko M.N., Mostowoj A.S.** (1970), Konstrukcja samolotów, *Wydawnictwo Komunikacji i Łączności*, Warszawa.
16. **Szymczyk E.** (2010), Numeryczna analiza deformacji nitu grzybkowego i otworu nitowego w procesie zakuwania, *Biuletyn WAT* 4.
17. **Szymczyk E., Jachimowicz J.** (2007), Analiza powierzchni kontaktu w połączeniu nitowym, *Biul. WAT* Vol. LVI Nr 4.
18. **Szymczyk E., Orzyłowski M.** (2010), Numerical modelling of a selected part of the airplane fuselage, Journal of KONES, Vol. 17, nr 2, 459-465, *European Science Society of Powertrain and Transport Publication*, Warszawa.